

Original Article

## Electrochemical studies on corrosion resistance of phosphate chemical conversion coatings on low carbon steel API 5L grade B

Vahid Asadi, Iman Danaee\*, Hadi Eskandari, and Soudabeh Nikmanesh

<sup>1</sup> Faculty of Petroleum Engineering, Petroleum University of Technology, Abadan, Iran

Received: 12 April 2016; Revised: 4 November 2016; Accepted: 8 November 2016

### Abstract

Zinc phosphate chemical conversion coatings was formed on low carbon steel (API 5L grade B) from nitrate bath and the corrosion performance of coatings was investigated using potentiodynamic polarization and electrochemical impedance spectroscopy studies. The characterization and composition of coatings were studied by SEM and EDS analysis in different immersion times. The corrosion resistance in 3.5 %wt. NaCl solution increased in the presence of zinc phosphate conversion coatings. The effect of immersion time and coating temperature were investigated on anti-corrosion behavior of coatings. Coating temperature indicated a significant effect in phosphate conversion coating and higher corrosion resistance was obtained with 70 °C operating temperature. Also the experimental results showed the increase in corrosion resistance with increasing the immersion time. This behavior can be due to the increase of the phosphate coating continuity and which formed on the surface. Surface analysis results indicated that uniform and continuous coating was obtained in agreement with electrochemical techniques.

**Keywords:** annual-ring, leaf phenology, monthly wood increment, *Melia azedarach*, path analysis (PA)

### 1. Introduction

Even with advanced corrosion resistant materials available, carbon steel has been widely employed as construction materials for pipe work in the oil and gas production such as down hole tubular, flow lines, chemical processing, petroleum production and refining and transmission pipelines. Steel pipelines play an important role in transporting gases and liquids throughout the world (Forero *et al.*, 2014; Jafari *et al.*, 2013). Different effective methods have been used to control corrosion including inhibitors, applying anodic/cathodic protection, coatings and proper design (Bahri *et al.*, 2014). An effective technique to solve the problem is surface treatment, which includes chemical conversion coating, electroplating and electroless plating, physical vapor deposition and so on (Bahri *et al.*, 2014; Kazemi *et al.*, 2014; Lazar *et al.*, 2014; Tomachuk *et al.*, 2014). Chemical conversion coatings are a simple and cost effective method and have been increasingly used in a wide range of applications.

The most widely used metal pre-treatment process for the surface treatment and finishing of ferrous and non-ferrous metals is phosphate conversion coatings (Arthanareeswari *et al.*, 2010; Jegannathan *et al.*, 2005, 2006a, 2006b; Sankara Narayanan *et al.*, 2006). The phosphate conversion coatings have popularity because of its ability to prevent under film corrosion and to improve adhesion of the organic topcoat (Kouisni *et al.*, 2005). Phosphating increases paint adhesion, corrosion resistance and promotes electrical insulation (Sheng *et al.*, 2011). Zinc, iron, and manganese phosphate are the most commonly phosphate coatings for corrosion protection (Jegannathan *et al.*, 2005, 2006a, b).

Phosphate coating starts after immersing the metal in a solution containing soluble primary metal phosphates, free phosphoric acid, various accelerators and modifiers (Bikulcius *et al.*, 2003). This process is a chemical reaction. In the zinc phosphating of carbon steel, iron will be dissolved at microanodic sites due to the presence of phosphoric acid in bath. pH increases in the metal solution interface due to hydrogen evolution on microcathodic sites. This leads to equilibrium between the soluble primary phosphates to insoluble tertiary phosphate on the surface. For repressing the

\*Corresponding author  
Email address: danaee@put.ac.ir

hydrolysis and keeping the bath stable, a certain amount of free phosphoric acid must be present in bath for effective deposition of phosphate at the microcathodic sites (Jegannathan *et al.*, 2005, 2006a; Sankara Narayanan *et al.*, 2006). Kavitha *et al.* (2014) studied the deposition of zinc–zinc phosphate composite coatings on steel by cathodic electrochemical treatment and indicated that the proportions of zinc and zinc phosphate could be varied with applied current density, pH, and treatment time. Temperature and immersion time are main effective parameters in zinc phosphate conversion coatings. In our previous work (Asadi *et al.*, 2015) the effect of temperature and immersion times was investigated for phosphate conversion coatings. Effect of copper (II) acetate pretreatment was investigated on zinc phosphate coating morphology and corrosion resistance (Abdalla *et al.*, 2013). The pretreatment resulted in a compact and uniform phosphate coating with higher corrosion resistance for mild steel. Diaz *et al.* (2015) investigated the corrosion protective properties of zinc phosphate coatings deposited on high strength steel under different operating conditions and showed that the use of ultrasonic vibration during the phosphating process promotes modifications in the phosphate crystal growth and, consequently improved corrosion resistance. However, the knowledge of periodic wood formation in other tropical tree species in Thailand is still rare and raises the question of which species forming the true annual-ring and responding to climate are not yet solved. In order to improve the limitations of the tropical tree-ring studies, it is essential to explore the information of which tree species is potentially available for climate-growth responses and annual-ring analysis. Fritts (1976) explained the general growth model of the trees as the relationship of climate and annual growth periodicity in terms of phenology and wood increments. By using a modified method of cambial wounding with Mariaux's windows (Mariaux, 1967), a technique to detect the annual growth periodicity in the wood, the mature white cedar trees (*Melia azedarach* L.) illustrating a distinct growth ring, which the information of periodic wood and annual-ring formations still lacked and the potential for annual-ring analysis involved climate variability was not studied yet, were selected to investigate annual-ring formation association with other factors described in the general growth model of the trees in order to study the potential for climate-growth responses.

In this work, chemical method was used for zinc phosphate conversion coating deposition on carbon steel in different temperatures and immersion times in the presence of sodium nitrate as an oxidative accelerator. The surface morphology of phosphate coating samples was investigated by scanning electron microscope (SEM) and the composition of the coating surface was evaluated by EDS analysis in different immersion times. Corrosion resistance of these coatings was studied by polarization curve and electrochemical impedance spectroscopy (EIS) in 3.5% sodium chloride solution.

## 2. Experimental Details

### 2.1. Deposition of zinc phosphate coating

Carbon steel substrates with composition: C: 0.086, P: 0.011, S: 0.002, Cu: 0.014, Al: 0.015, N: 0.076, V: 0.001,

Ti: 0.008, Mo: 0.001, Mn: 1.35, Cr: 0.009 %w, Fe: Rest, were prepared from Ahvaz Pipe Mills Company for deposition of phosphate coatings. The compositions of the phosphate baths used in this study were:  $\text{H}_3\text{PO}_4$  (25.5  $\text{gL}^{-1}$ ),  $\text{ZnO}$  (10  $\text{gL}^{-1}$ ),  $\text{HNO}_3$  (5.88  $\text{gL}^{-1}$ ),  $\text{NaNO}_3$  (2  $\text{gL}^{-1}$ ) and pH=3 to 3.2. Immersion temperature was varied between 50 and 70 °C and different immersion times 5, 10, 20 and 30 min were used for phosphate conversion coatings.

Specimens were cut to 1 cm × 1 cm samples from larger panels. Prior to surface pretreatments process, all samples were mounted in polymeric resin and the surface of 1  $\text{cm}^2$  was obtained. The samples were mechanically abraded with abrasive papers. Then, the specimens were rinsed with deionized water and immersed in the bath that maintained at special temperature for particular time, immediately. A gray coating with bright crystalline spots was formed on the substrate. After phosphate conversion coatings, the coated samples were rinsed with deionized water and acetone to remove residual acid and salts from the bath and then exposed to ambient temperature for some hours.

### 2.2. Evaluating of corrosion performance

Potentiodynamic polarization and electrochemical impedance spectroscopy (EIS) were carried out by Autolab PGSTAT 302N instrument. A three electrode cell containing a 3.5% NaCl solution at room temperature with Pt as counter and saturated Ag/AgCl as reference electrode was employed for this measurements. Potentiodynamic polarization measurements were carried out with potential scan rate of  $1\text{mVs}^{-1}$ . Electrochemical impedance was done at open circuit potential with AC amplitude of 10 mV over a frequency range of 100 kHz to 1 mHz. Fitting of experimental impedance spectroscopy data to the proposed equivalent circuit was done by means of a home written least square software based on the Marquardt method for the optimization of functions and Macdonald weighting for the real and imaginary parts of the impedance (Danaee, 2011; Macdonald, 1984).

### 2.3. Surface characteristics of coating

The color of the zinc phosphate coatings in visual appearance was grayish with bright crystalline spots. Scanning electron microscope (SEM) model VGEA\ TESCAN equipped with energy dispersive X-ray EDX analysis was used to investigate the surface morphology of zinc phosphate coated steel and the composition of the coating surface.

## 3. Results and Discussion

### 3.1. Effect of different temperature on corrosion performance

Figure 1 shows the polarization curves of steel electrode without and with phosphate coatings in 3.5% NaCl solution. Coatings were obtained by 20 min immersion time in the phosphating bath at different temperature. The electrochemical data including corrosion potential ( $E_{corr}$ ), corrosion current density ( $I_{corr}$ ), cathodic and anodic Tafel slopes ( $\beta_a, \beta_c$ ), polarization resistance ( $R_p$ ) of each sample are shown in Table1. It should be noted that the results

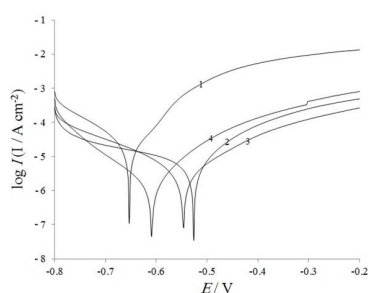


Figure 1. Polarization curves of steel electrode with and without zinc phosphate conversion coatings. Conversion coatings were obtained by 20 min immersion time in phosphate solution in different temperatures: 1) uncoated, 2) 50 °C, 3) 60 °C, 4) 70 °C.

are calculated by using Tafel extrapolation method. The Stern-Geary equation (Equation 1) is used to calculate the  $R_p$  (Danaee *et al.*, 2015; Gholami *et al.*, 2013):

$$I_{corr} = (1/2.303R_p) (B_a B_c / B_a + B_c) \quad (1)$$

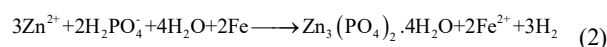
Table 1. Potentiodynamic polarization parameters of different operating temperature for the phosphate coatings in 3.5 wt. % NaCl solution. Coatings were prepared by 20 min immersion time in phosphate solution.

Phosphate Coating	$B_a$ / V dec <sup>-1</sup>	$B_c$ / V dec <sup>-1</sup>	$I_{corr}$ / A cm <sup>-2</sup>	$E_{corr}$ / V	$R_p$ / ohm	Corr. rate / mpy
Uncoated	0.114	0.094	$2.8 \times 10^{-5}$	-0.653	772.995	$3.39 \times 10^{-1}$
50 °C, 20 min	0.241	0.087	$4.9 \times 10^{-6}$	-0.526	5617.637	$5.80 \times 10^{-2}$
60 °C, 20 min	0.146	0.121	$3.0 \times 10^{-6}$	-0.547	9532.126	$3.54 \times 10^{-2}$
70 °C, 20 min	0.097	0.082	$1.4 \times 10^{-6}$	-0.609	13635.849	$1.66 \times 10^{-2}$

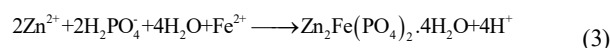
These coatings provide an effective physical barrier to protect metals and significantly decrease the corrosion rate due to the insulating nature of phosphate conversion coatings. In NaCl solution, the predominant reactions that could occur during the cathodic and anodic polarization are the reduction of oxygen and iron dissolution, respectively (Jegannathan *et al.*, 2006a, b). Phosphate coated samples shows lower corrosion current density, higher polarization resistance and more positive corrosion potential (Figure 1). According to these data, the corrosion resistance of carbon steel increases in the presence of the phosphating treatment. In addition, the anodic and cathodic processes of carbon steel corrosion are suppressed effectively by complete coverage of phosphate coatings. However, the influence is more pronounced in the anodic polarization plots compared to that in the cathodic polarization plots. It is clear that in the presence of phosphate, iron dissolution reaction decreases to a greater extent when compared to cathodic reaction and therefore, the  $E_{corr}$  values shift to the more positive side in the presence of phosphate.

As shown in Table 1, the phosphate coatings prepared at higher temperatures show the higher polarization resistance and the lower corrosion current density. According

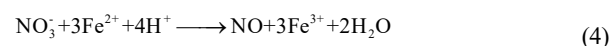
to the literature (Satoh, 1987; Rausch, 1990; Losch *et al.*, 1994) Equation 2 summarizes the whole process:



The zinc phosphate coating consists mainly of Hopeite  $\text{Zn}_3(\text{PO}_4)_2 \cdot 4\text{H}_2\text{O}$  as the top layer, although it is proved that a mixed Fe/Zn compound can be formed as well at the beginning of the phosphating process in steel substrates, Equation 3. The  $\text{Fe}^{2+}$  ions come from the pickling reaction. This Fe/Zn compound, called phosphor phyllite, is mainly detected at the innermost part of the phosphate layer (Rausch, 1990; Sankara, 2005).



It was reported phosphating had slow reaction, since the high operating temperature increases the rate of reaction (Fouladi & Amadeh, 2013). Although the reactions occur at low temperatures but their kinetics are so slow and therefore higher temperatures results in more formation of phosphate phases specially Hopeite (Ashassi-Sorkhabi *et al.*, 2007). In addition, increase in temperature leads to an increase in extent of metal dissolution which causes more crystals formation and compact structure of coating. In comparison with previous work (Asadi *et al.*, 2015), the corrosion current is lower in the presence of oxidative accelerator in phosphating bath with the same immersion times and decreases from  $6.49 \times 10^{-6}$  to  $1.41 \times 10^{-6}$  A cm<sup>-2</sup> in optimum condition. The accelerators  $\text{NaNO}_3$  promotes iron oxidation and can oxidize ferrous cations resulting in the formation of  $\text{FePO}_4$  (Losch *et al.*, 1993). The reaction of such a process is described by Equation 4:



This reaction involves lowering of the hydrogen ion concentration at the substrate/solution interface, increasing the local interfacial pH, and promoting then the Zn-phosphate precipitation. The so-formed solid phase,  $\text{FePO}_4$ , is only slightly soluble in acid media and thus will provide further corrosion resistance if it remains as a layer at the bottom of the uncovered surface.

Electrochemical impedance was used to get more information about the anticorrosion behavior of the phosphate coating. The Nyquist plots of zinc phosphated steel obtained by 20 min immersion in phosphate solution in different operating temperatures are presented in Figure 2a. Impedance was measured at open circuit potential (OCP) in 3.5 %wt. NaCl solution. The data indicate that the impedance diagrams consist of a depressed capacitive loop which is due to the double layer capacitance and charge transfer resistance. The equivalent circuit compatible with the Nyquist diagram is depicted in Figure 2b. The simplest approach requires the theoretical transfer function  $Z(\omega)$  to be represented by a parallel combination of a resistance  $R_{ct}$  and a capacitance  $C_{dl}$ , both in series with another resistance  $R_s$  according to Equation 5 (Danaee *et al.*, 2011):

$$Z(\omega) = R_s + \frac{1}{1/R_{ct} + i\omega C_{dl}} \quad (5)$$

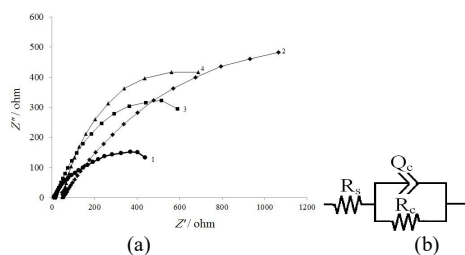


Figure 2. a) Nyquist plots of steel electrode with and without zinc phosphate conversion coatings. Conversion coatings were obtained by 20 min immersion time in phosphate solution in different temperatures: 1) uncoated, 2) 50 °C, 3) 60 °C, 4) 70 °C. b) Equivalent circuits compatible with the experimental impedance data for corrosion of zinc phosphate coated steel electrode.

where  $\omega$  is the frequency in rad/s,  $\omega = 2\pi f$  and  $f$  is frequency in Hz. To obtain a satisfactory impedance simulation of phosphate coated steel, it is necessary to replace the capacitor (C) with a constant phase element (CPE) Q in the equivalent circuit. The most widely accepted explanation for the presence of CPE behavior and depressed semicircles on solid electrodes is microscopic roughness, causing an inhomogeneous distribution in the solution resistance as well as in the double-layer capacitance (Karimi *et al.*, 2015; Ramesh Kumar *et al.*, 2015). In electrical equivalent circuit,  $R_s$ ,  $Q_{dl}$  and  $R_{ct}$  represent solution resistance, a constant phase element corresponding to the double layer capacitance and the charge transfer resistance, respectively.

To corroborate the equivalent circuit, the experimental data were fitted to equivalent circuit and the circuit elements were obtained. The equivalent circuit parameters for the impedance spectra of phosphate coated steel in NaCl solution are shown in Table 2. The charge transfer resistances of the zinc phosphated samples significantly increase. Moreover, higher corrosion resistance is obtained with 70 °C coating temperature. The low value of  $C_{dl}$  reveals the decrease in exposed area of electrode due to phosphate coatings (Danace *et al.*, 2015). The  $Q_{dl}$  exponent ( $n$ ) is a measure of the surface heterogeneity, and the low value indicates that the constant phase element is different from perfect capacitance. The values of  $n$  in Table 2 illustrate that the electrode surface becomes more homogeneous in the higher coating temperature.

Table 2. Impedance parameters of different operating temperature for the phosphate coatings in 3.5 wt. % NaCl solution. Coatings were prepared by 20 min immersion time in phosphate solution.

Phosphate coating	$R_{ct}$ / ohm	$Q$ / F	$n$
uncoated	605	0.015	0.61
50°C, 20 min	1435	0.008	0.65
60°C, 20 min	931	0.009	0.75
70°C, 20 min	1618	0.01	0.74

### 3.2. Effect of immersion time on corrosion Performance

Figure 3 presents the polarization curves of phosphate coatings obtained in different immersion time in the

phosphating bath at 70°C. Table 3 illustrates the corresponding corrosion parameters in 3.5% NaCl solution. As can be seen,  $I_{corr}$  and corrosion rate of the coated samples decrease by increasing immersion time from 5 to 20 min. But in higher immersion times, 30 min, corrosion current density and corrosion rate increases. In low immersion time, the surface is attacked by  $H^+$  ions presented in phosphating bath and the conversion coating formation is in the induction stage (Fouladi & Amadeh, 2013). This leads to increasing the corrosion rate. Therefore, weak coating forms at this immersion time, and also, the carbon steel surface is corroded. By increasing the immersion time, the phosphate layer has enough time to settle on the steel surface, and produce a proper thickness for corrosion protection. Zinc and Iron phosphate coats steel surface completely in this immersion time. But if the immersion time is too long, the quality and protective properties of coating reduces due to agglomeration and extra growth of phosphate crystals in the coating. This leads to the internal stress which decreases its toughness and increases porosity and cracking. Also, with increasing immersion times, the thickness of phosphate conversion coatings increases and therefore cracked and porous structures are attributed to the drying process. The upper layer of the coating will be hardened during drying process and water was trapped in inner phosphate layer. So the trapped water cannot release from the coating because of the presence of the top hard layer and lead to porosity and cracking. In addition to increasing thickness, some phosphophyllite-hopeite phase conversion is occurred with increasing immersion times which will be investigated by energy dispersive X-ray technique.

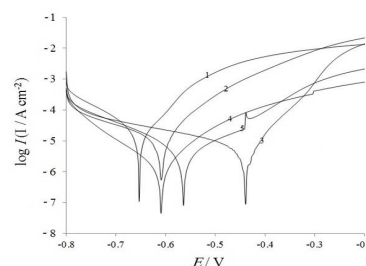


Figure 3. Polarization curves of steel electrode with and without zinc phosphate conversion coatings. Conversion coatings were obtained at 70 °C in phosphate solution with different immersion times: 1) uncoated, 2) 5 min, 3) 10 min, 4) 20 min, 5) 30 min.

Table 3. Potentiodynamic polarization parameters of different immersion times for the phosphate coatings in 3.5 wt. % NaCl solution. Coatings were prepared by immersion in phosphate solution in 70 °C.

Phosphate Coating	$B_a$ / V dec <sup>-1</sup>	$B_c$ / V dec <sup>-1</sup>	$I_{corr}$ / A cm <sup>-2</sup>	$E_{corr}$ / V	$R_p$ / ohm	Corr. rate / mpy
uncoated	0.114	0.094	$2.89 \times 10^{-5}$	-0.653	772.995	$3.39 \times 10^{-1}$
70°C, 5 min	0.186	0.084	$1.18 \times 10^{-5}$	-0.610	2125.774	$1.38 \times 10^{-1}$
70°C, 10 min	0.248	0.067	$5.44 \times 10^{-6}$	-0.439	4209.624	$6.39 \times 10^{-2}$
70°C, 20 min	0.097	0.082	$1.41 \times 10^{-6}$	-0.609	13635.849	$1.66 \times 10^{-2}$
70°C, 30 min	0.121	0.136	$3.57 \times 10^{-6}$	-0.564	7768.470	$4.20 \times 10^{-2}$

Figure 4 illustrates the Nyquist plots at OCP for the phosphate conversion coating obtained by 70°C operating temperature in different immersion times. All coatings indicate capacitive loop attributed to the charge transfer resistance and double layer capacitance. The experimental data were fitted to the equivalent circuit (Figure 2b) and the circuit elements were obtained. The equivalent circuit parameters for the impedance spectra of the phosphate coated steel obtained in different immersion times are shown in Table 4. The charge transfer resistance increases in the presence of phosphate coatings. In addition, with increasing immersion times, the corrosion resistance increases due to the completion of phosphate layer. As can be seen, higher corrosion resistance is obtained in 20 min immersion time. This is in agreement with the potentiodynamic polarization data.

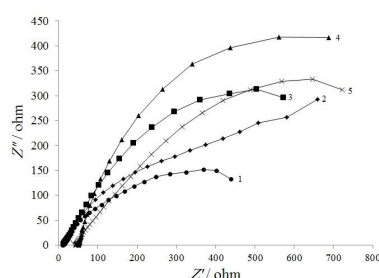


Figure 4. Nyquist plots of steel electrode with and without zinc phosphate conversion coatings. Conversion coatings were obtained at 70 °C in phosphate solution with different immersion times: 1) uncoated, 2) 5 min, 3) 10 min, 4) 20 min, 5) 30 min.

Table 4. Impedance parameters of different immersion times for the phosphate coatings in 3.5 wt. % NaCl solution. Coatings were prepared by immersion in phosphate solution in 70 °C.

Phosphate coating	$R_{ct}$ / ohm	$Q$ / F	$n$
uncoated	605	0.015	0.61
70°C, 5 min	1332	0.012	0.51
70°C, 10 min	934	0.017	0.71
70°C, 20 min	1618	0.01	0.74
70°C, 30 min	1108	0.015	0.69

### 3.3. Morphology and composition of the coating

Figure 5 illustrates the SEM images and EDX analysis of phosphate conversion coatings obtained by 70°C operating temperature indifferent immersion times in phosphate solution and the corresponding elemental analysis is shown in Table 5. It can be seen that in low immersion time, the formation of phosphate coating is in the induction stage and incomplete phosphate coating forms. Moreover, the surface is attacked by phosphoric acid and causes the inferior corrosion behavior (Figure 5a). As indicated in Figure 5b, with increasing immersion time, the phosphate crystals grow and uniform and compact coating is obtained. In the very high immersion time (Figure 5c), the more growth is observed in phosphate crystals and coarse crystal and heavy deposit of coating is created in SEM image. This can be an evidence of high growth of crystal grains in coating which creates internal

force between grains and more external growth of coating. This leads to stress between crystal grains and decreasing the corrosion resistance. In addition, extra growth of under layers of crystal causes the disorder in upper layer of the phosphate coatings and leads to lower internal compactness. Figure 5d-f illustrates the EDX analysis of zinc phosphate coated steel electrode obtained by in different immersion.

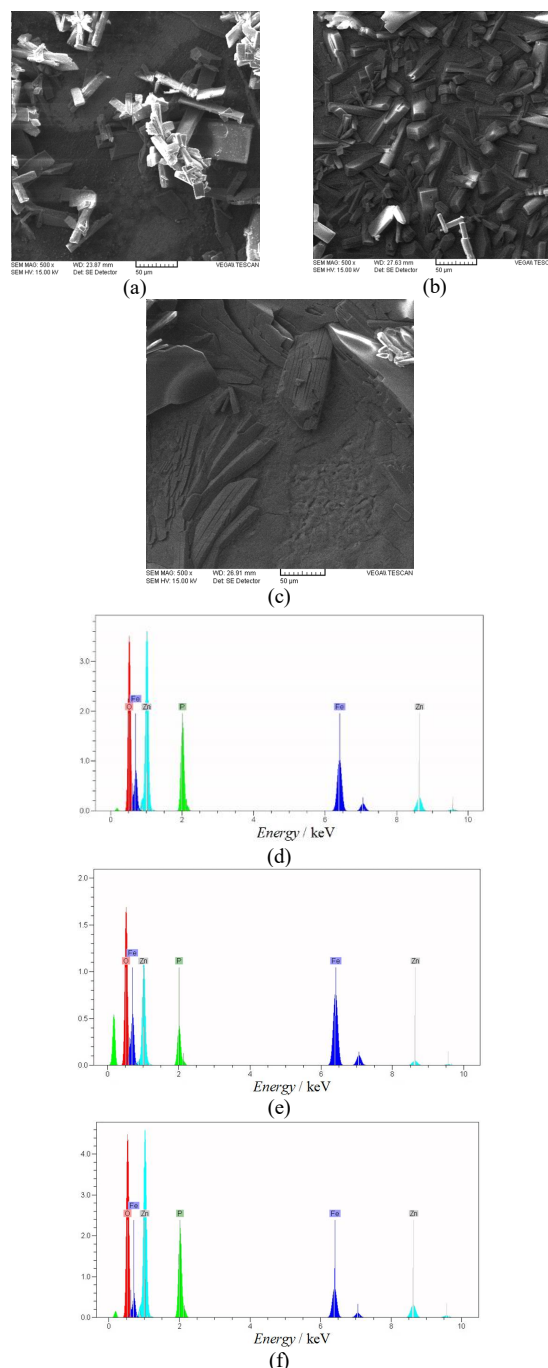


Figure 5. SEM images and EDS spectra of zinc phosphate conversion coatings obtained at 70 °C in phosphate solution with different immersion times: a) SEM, 5 min, b) SEM, 20 min, c) SEM, 30 min, d) EDX, 5 min, e) EDX, 20 min and f) EDX, 30 min.

Table 5. Elemental compositions of zinc phosphated samples obtained by EDS analysis.

Sample	oxygen	Phosphorus	Iron	Zinc	Zn/Fe
70°C, 5 min	30.12	5.36	53.16	11.36	0.21
70°C, 20 min	26.31	10.53	36.42	26.73	0.73
70°C, 30 min	36.61	11.89	21.02	30.49	1.45

According to Table 5, phosphorous and zinc increases with increasing immersion times and iron decreases which indicates increasing thickness and weight of phosphate conversion coatings. Moreover, the increase in weight ratio of Zinc/Iron is due to the increase of Hopeite ratio in comparison with phosphophyllite phase with increasing immersion times which shows phase conversion in phosphate coatings in acidic solution with increasing immersion times.

#### 4. Conclusions

The corrosion behavior of phosphate conversion coatings applied on steel surface was investigated in 3.5 wt. % NaCl solution. This conversion coating improved the corrosion resistance of the steel due to the formation of barrier film. The potentiation dynamic polarization studies showed that the anodic and cathodic currents decreased and the polarization resistance increased in the presence of zinc phosphating. The phosphating temperature played an important role to provide phosphate conversion coating and the higher corrosion resistance was obtained in higher operating temperature. In addition, the corrosion resistance increased with increasing the immersion time due to the increasing of the phosphate coating continuity and compactness. The results of SEM showed that the phosphate coatings, obtained from 20 min immersion time in 70 °C operating temperature, were more uniform and continuous.

#### References

- Abdalla, K., Rahmat, A., & Azizan, A. (2013). Effect of copper (II) acetate pretreatment on zinc phosphate coating morphology and corrosion resistance. *Journal of Coatings Technology and Research*, 10, 133-139.
- Arthanareeswari, M., Sankara Narayanan, T. S. N., Kamaraj, P., & Tamilselvi, M. (2010). Influence of galvanic coupling on the formation of zinc phosphate coating. *Indian Journal of Chemical Technology*, 17, 167-175.
- Asadi, V., Danaee, I., & Eskandari, H. (2015). The effect of immersion time and immersion temperature on the corrosion behavior of zinc phosphate conversion coatings on carbon steel. *Materials Research*, 18, 706-713.
- Ashassi-Sorkhabi, H., Seifzadeh, D., & Harrafi, H. (2007). Phosphatation of iron powder metallurgical samples for corrosion protection. *Journal of Iranian Chemical Society*, 4, 72-77.
- Bahri, H., Danaee, I., & Rashed, G. R. (2014). The effect of curing time and curing temperature on the corrosion behavior of nanosilica modified potassium silicate coatings on AA2024. *Surface and Coatings Technology*, 254, 305-312.
- Bikulcius, G., Burokas, V., Martusiene, A., & Matulionis, E. (2003). Effects of magnetic fields on the phosphating process. *Surface and Coatings Technology*, 172, 139-143.
- Danaee, I. (2011). Kinetics and mechanism of palladium electrodeposition on graphite electrode by impedance and noise measurements. *Journal of Electroanalytical Chemistry*, 662, 415-420.
- Danaee, I., Gholami, M., RashvandAvei, M., & Maddahy, M. H. (2015). Quantum chemical and experimental investigations on inhibitory behavior of amino-iminotautomeric equilibrium of 2-aminobenzothiazole on steel corrosion in H<sub>2</sub>SO<sub>4</sub> solution. *Journal of Industrial and Engineering Chemistry*, 26, 81-94.
- Díaz, B., Freire, L., Mojó, M., & Nóvoa, X. R. (2015). Optimization of conversion coatings based on zinc phosphate on high strength steels, with enhanced barrier properties. *Journal of Electroanalytical Chemistry*, 737, 174-183.
- Forero, A. B., Núñez, M. M. G., & Bott, I. S. (2014). Analysis of the corrosion scales formed on API 5L X70 and X80 steel pipe in the presence of CO<sub>2</sub>. *Materials Research*, 17, 461-471.
- Fouladi, M., & Amadeh, A. (2013). Effect of phosphating time and temperature on microstructure and corrosion behavior of magnesium phosphate coating. *Electrochimica Acta*, 106, 1-12.
- Gholami, M., Danaee, I., Maddahy, M. H., & RashvandAvei, M. (2013). Correlated ab initio and electroanalytical study on inhibition behavior of 2-mercaptobenzothiazole and its thiole-thionetautomerism effect for the corrosion of steel (api 5l x52) in sulphuric acid solution. *Industrial and Engineering Chemistry Research*, 52, 14875-14889.
- Jafari, H., Danaee, I., Eskandari, H., & RashvandAvei, M. (2013). Electrochemical and quantum chemical studies of N,N-bis(4-hydroxybenzaldehyde)-2,2-dimethylpropandiimine Schiff base as corrosion inhibitor for low carbon steel in HCl solution. *Journal of Environmental Science and Health, Part A*, 48, 1628-1641.
- Jafari, H., Danaee, I., Eskandari, H., & RashvandAvei, M. (2013). Electrochemical and Theoretical Studies of Adsorption and Corrosion Inhibition of N,N'-Bis(2-hydroxyethoxyacetophenone)-2,2-dimethyl-1,2-propanediimine on Low Carbon Steel (API 5L Grade B) in Acidic Solution. *Industrial and Engineering Chemistry Research*, 52, 6617-6632.
- Jamali, F., Danaee, I., & Zaarei, D. (2015). Effect of nano-silica on the corrosion behavior of silicate conversion coatings on hot-dip galvanized steel. *Materials and Corrosion*, 66, 459-464.
- Jegannathan, S., Sankara Narayanan, T. S. N., Ravichandran, K., & Rajeswari, S. (2005). Performance of zinc phosphate coatings obtained by cathodic electrochemical treatment in accelerated corrosion tests. *Electrochimica Acta*, 51, 247-256.
- Jegannathan, S., Sankara Narayanan, T. S. N., Ravichandran, K., & Rajeswari, S. (2006a). Evaluation of the corrosion resistance of phosphate coatings obtained by anodic electrochemical treatment. *Progress in organic coatings*, 57, 392-399.



- Jegannathan, S., Sankara Narayanan, T. S. N., Ravichandran, K., & Rajeswari, S. (2006b). Formation of zinc phosphate coating by anodic electrochemical treatment. *Surface and Coatings Technology*, 200, 6014-6021.
- Karimi, A., Danaee, I., Eskandari, H., & RashvanAvei, M. (2015). Electrochemical investigations on the inhibition behavior and adsorption isotherm of synthesized di-(resacetophenone)-1,2-cyclohexanediimine schiff base on the corrosion of steel in 1 m HCL. *Protection of Metals and Physical Chemistry of Surfaces*, 51, 899-907.
- Kavitha, C., Narayanan, T. S. N. S., Ravichandran, K., Park, I. S., & Lee, M. H. (2014). Deposition of zinc-zinc phosphate composite coatings on steel by cathodic electrochemical treatment. *Journal of Coatings Technology and Research*, 11, 431-442.
- Kazemi, M., Danaee, I., & Zaarei, D. (2014). The effect of pre-anodizing on corrosion behavior of silicate conversion coating on AA2024. *Materials Chemistry and Physics*, 148, 223-229.
- Kouisni, L., Azzi, M., Dalard, F., & Maximovitch, S. (2005). Phosphate coatings on magnesium alloy AM60 Part 2: Electrochemical behaviour in borate buffer solution. *Surface and Coatings Technology*, 192, 239-246.
- Lazar, A. M., Yespica, W. P., Marcelin, S., Pèbère, N., Samélor, D., Tendero, C., & Vahlas, C. (2014). Corrosion protection of 304L stainless steel by chemical vapor deposited alumina coatings. *Corrosion Science*, 81, 125-131.
- Losch, A., Klusmann, E., & Schultze, J. W. (1994). Electrochemical investigations of phosphate layers by metal deposition and cataphoretic painting. *ElectrochimicaActa*, 39, 1183-1187.
- Losch, A., & Schultze, J. W. (1993). Impedance spectroscopy and other electrochemical in-situ investigations of the phosphating process. *Journal of Electro-analytical Chemistry*, 359, 39-61.
- Macdonald, J. R. (1984). Note on the parameterization of the constant phase admittance Element. *Solid State Ionics*, 13, 147-149.
- Medvedeva, M. L., Ratanova, M. D., & Barat, V. A. (2015). Acoustic emission in monitoring corrosion of crude distillation-unit equipment. *Chemical and Petroleum Engineering*, 51, 574-577.
- RameshKumar, S., Danaee, I., RashvandAvei, M., & Vijayan, M. (2015). Quantum chemical and experimental investigations on equipotent effects of (+)R and (-)S enantiomers of racemic amisulpride as eco-friendly corrosion inhibitors for mild steel in acidic solution. *Journal of Molecular Liquids*, 212, 168-186.
- Rausch, W. (1990). *The phosphating of metals*. Ohio, OH: ASM International.
- Sankara, T. S. N. (2005). Surface pretreatment by phosphate conversion coatings. *Advanced Materials Science*, 9, 130-177.
- Sankara Narayanan, T. S. N., Jegannathan, S., & Ravichandran K. (2006). Corrosion resistance of phosphate coatings obtained by cathodic electrochemical treatment: Role of anode-graphite versus steel. *Progress in Organic Coatings*, 55, 355-362.
- Satoh, N. (1987). Effects of heavy metal additions and crystal modification on the zinc phosphating of electro-galvanized steel sheet. *Surface and Coatings Technology*, 30, 171-181.
- Sheng, M., Wang, Y., Zhong, Q., Wu, H., Zhou, Q., & Lin H. (2011). The effects of nano-SiO<sub>2</sub> additive on the zinc phosphating of carbon steel. *Surface and Coatings Technology*, 205, 3455-3460.
- Tomachuk, C. R., Elsner, C. I., & Di Sarli, A. R. (2014). Electrochemical characterization of chromate free conversion coatings on electrogalvanized steel. *Materials Research*, 17, 61-68.